

Tethering of ferredoxin:NADP⁺ oxidoreductase to thylakoid membranes is mediated by novel chloroplast protein TROL

Snježana Jurić¹, Kroata Hazler-Pilepić², Ana Tomašić¹, Hrvoje Lepeduš³, Branka Jeličić¹, Sujith Puthiyaveetil⁴, Tihana Bionda⁵, Lea Vojta¹, John F. Allen⁴, Enrico Schleiff⁵ and Hrvoje Fulgosi^{1,*}

¹Department of Molecular Biology, Ruđer Bošković Institute, Bijenička cesta 54, HR-10000 Zagreb, Croatia,

²Department of Pharmaceutical Botany, Faculty of Pharmacy and Biochemistry, University of Zagreb, Schrottova 39, HR-10000 Zagreb, Croatia,

³Agricultural Institute Osijek, Južno predgrađe 17, HR-31000 Osijek, Croatia,

⁴School of Biological and Chemical Sciences, Queen Mary, University of London, Mile End Road, London E1 4NS, UK, and

⁵JWGU Frankfurt am Main, Cluster of Excellence Macromolecular Complexes, Department of Biosciences, Max-von-Laue Street 9, D-60439 Frankfurt, Germany

Received 9 June 2009; revised 24 July 2009; accepted 4 August 2009; published online 9 September 2009.

*For correspondence (fax +385 1 45 61 177; e-mail fulgosi@irb.hr).

SUMMARY

Working in tandem, two photosystems in the chloroplast thylakoid membranes produce a linear electron flow from H₂O to NADP⁺. Final electron transfer from ferredoxin to NADP⁺ is accomplished by a flavoenzyme ferredoxin:NADP⁺ oxidoreductase (FNR). Here we describe TROL (thylakoid rhodanese-like protein), a nuclear-encoded component of thylakoid membranes that is required for tethering of FNR and sustaining efficient linear electron flow (LEF) in vascular plants. TROL consists of two distinct modules; a centrally positioned rhodanese-like domain and a C-terminal hydrophobic FNR binding region. Analysis of Arabidopsis mutant lines indicates that, in the absence of TROL, relative electron transport rates at high-light intensities are severely lowered accompanied with significant increase in non-photochemical quenching (NPQ). Thus, TROL might represent a missing thylakoid membrane docking site for a complex between FNR, ferredoxin and NADP⁺. Such association might be necessary for maintaining photosynthetic redox poise and enhancement of the NPQ.

Keywords: ferredoxin:NADP⁺ oxidoreductase (FNR), high-light, linear electron flow, retrograde signalling, rhodanases.

INTRODUCTION

Efficient photosynthetic energy conversion requires a high degree of integration and regulation of various redox reactions in order to maximize the use of available light and to minimize damaging effects of excess light (Allen, 2002). The interplay between cyclic (CEF), linear and pseudocyclic electron transport pathways is required for maintaining the poised state of the photosynthetic system (Allen, 2003). In the over-oxidized state there is no electron flow, while in the over-reduced state photooxidation can cause damage to photosystems and eventually death. Common to all three pathways is the activity of PSI that transfers electrons from the lumen-located plastocyanin to the stromal ferredoxin (Fd). This transfer is mediated by three subunits, C, D and E, of the so-called stromal ridge of PSI (Nelson and Yocum, 2006). Fd in the reduced state (Fd_{red}) provides electrons for the ferredoxin:NADP⁺ oxidoreductase (FNR), which pro-

duces NADPH in a linear pathway (Carrillo and Ceccarelli, 2003), for the ferredoxin–thioredoxin reductase (FTR), which catalyses the reduction of chloroplast thioredoxins (Shadong *et al.*, 2007), for feeding of the CEF (Allen, 2003) or, alternatively, electrons can be transferred to superoxide, the terminal acceptor in pseudocyclic pathway (Allen, 2003).

Proteins involved in electron transfer often participate in different reactions in which they have to interact with various other proteins (Medina and Gómez-Moreno, 2004). Due to the variability of interacting surfaces it is reasonable to assume that there are complexes that are tighter binding, while others exhibit weaker interactions (Medina and Gómez-Moreno, 2004). It has been shown that FNR exists in soluble and membrane-bound forms (Palatnik *et al.*, 1997; Lintala *et al.*, 2007). FNR association with thylakoid membranes has been postulated to occur *via* PSI E subunit

(Andersen *et al.*, 1992), cytochrome *b₆/f* complex (Clark *et al.*, 1984; Zhang *et al.*, 2001) and in a complex with NADPH dehydrogenase (Quiles and Cuello, 1998). However, all these studies failed to unequivocally identify the exact protein partner responsible for FNR tethering.

In Arabidopsis, plastid-targeted FNR is encoded by a small multigene family in which two leaf-type FNR (AtLFNR1, AtLFNR2) and two root-type FNR isoenzymes are present (Hanke *et al.*, 2005). Both leaf-type isoforms are evenly distributed between the thylakoids and the soluble stroma and their exact functional differentiation remains to be elucidated. It has been proposed that formation of a heterodimer between the two leaf-type isoforms is required for membrane attachment of the AtLFNR2 (Lintala *et al.*, 2007). Recently, a third type of FNR, LFNR3, has been identified in maize leaves (Okutani *et al.*, 2005). Unlike the other two FNR types, LFNR3 is a soluble stroma protein (Okutani *et al.*, 2005). It is unclear why plastids require three types of FNR. It has been proposed that leaf FNR isoenzymes 1 and 2 are relatively more abundant under conditions of high demand for NADPH (Okutani *et al.*, 2005). Apart from leaf FNR isoforms, root plastids contain at least two additional FNR (RFNR) isoforms (Hanke *et al.*, 2005). It has been shown that multiple FNR isoenzymes have variable metabolic roles and differentially contribute to nitrogen assimilation (Hanke *et al.*, 2005).

Studies *in vivo* have revealed that suppression of FNR expression leads to increased susceptibility to photo-oxidative damage, impaired plant growth and lowered photosynthetic activity of transgenic plants (Hajirezaei *et al.*, 2002; Palatnik *et al.*, 2003). On the other hand, overexpression of FNR results in slightly increased rates of electron transport from water to NADP⁺ and increased tolerance to oxidative stress (Rodriguez *et al.*, 2007).

It has been demonstrated that the chloroplast inner envelope translocon protein Tic62 specifically anchors FNR (Küchler *et al.*, 2002). This interaction is mediated by a C-terminal domain which consists of three imperfect repeats. The FNR-binding domain of the Tic62-NAD(P)-related protein family can be found exclusively in vascular plants (Balsera *et al.*, 2007). The exact function of the FNR-Tic62 interaction is unknown, although it has been proposed to be involved in redox regulation of protein translocation into chloroplasts.

In recent years, many different proteins containing rhodanese (thiosulfate:cyanide sulfurtransferase) domains have been identified in the three major domains of life; bacteria, archaea and eukarya. Rhodanese domains are structurally related to the catalytic subunit of Cdc25 phosphatase enzymes. It is likely that two enzyme families share a common evolutionary origin (Bordo and Bork, 2002). It has been demonstrated that rhodanases catalyze the transfer of a sulfane sulfur atom from thiosulfate to cyanide *in vitro* (Mintel and Westley, 1966). Several rhodanese-like proteins

have been identified in various subcellular compartments of Arabidopsis (Bauer *et al.*, 2004). Although their exact function remains elusive, they have been implicated in processes of leaf senescence (Azumi and Watanabe, 1991) and plant immune response (Caplan *et al.*, 2008).

In this work we describe the identification of TROL, a rhodanese-like protein of photosynthetic membranes which is responsible for docking of FNR. Inactivation of TROL in the model plant Arabidopsis leads to a specific defect in efficiency of LEF.

RESULTS

Identification of the 66 kDa thylakoid auxiliary component

In order to isolate low-abundant protein components of photosynthetic machinery, we performed controlled detergent solubilization and subsequent precipitation of spinach thylakoids after removal of extrinsic proteins by a chaotropic wash. The resulting ammonium sulfate preparation (AMS) (Figure S1a) contains mostly cytochrome *b₆/f* components, several protein kinase activities and a number of low-abundant proteins (Sokolenko *et al.*, 1995). Upon separation on high-resolution SDS-PAGE, AMS polypeptides in the range between 45 and 66 kDa were subjected to N-terminal microsequencing. A polypeptide with an apparent molecular weight of 66 kDa (Figure S1b) was of particular interest as a BLAST search against the Arabidopsis genome resulted in identification of a locus At4g01050 with a unique molecular structure. Consensus predictions according to ARAMEMNON (Schwacke *et al.*, 2003) suggested an intrinsic transmembrane protein (Figure 1). The protein starts with less conserved ME dipeptide followed by serine and proline rich stretch and contains a hydrophobic domain (residues 49–66) close to its C-terminus. The terminal cleavage site consists of small side chain residues at –1 and –3, most likely A–X–S (von Heijne *et al.*, 1989). A centrally positioned domain of the polypeptide showed high sequence similarity to rhodanases (Figure 1). The NMR structure of the At4g01050 rhodanese-like domain has been previously determined (Pantoja-Uceda *et al.*, 2004, 2005). The analysed region spans 120 residues (from V175 to T295) and includes all features of rhodanese homology domain (Pantoja-Uceda *et al.*, 2004). The At4g01050 rhodanese-like domain lacks the active-site cysteine, which is replaced by an aspartate (Figure 1, indicated by a shaded box), consistent with the assumption that this domain represents an inactive rhodanese-like domain.

In vivo localization, import and membrane distribution of TROL

To test the assumption that the polypeptide is indeed synthesized as a precursor with the basic attributes for intracellular sorting, the At4g01050 ORF was fused in frame with the yellow fluorescent protein (YFP) reporter gene and the

Figure 1. Deduced amino acid sequence of the TROL precursor protein (At4g01050).

The arrow indicates the pre-sequence terminal cleavage site. The domain with high sequence similarity to rhodanases is centrally positioned, with the active-site cysteine exchanged by an aspartate, indicated by a shaded box. The possible PVP hinge domain (Sansom and Weinstein, 2000) is preceded with two bolded repeats rich in PVP motif. Transmembrane helices are assigned according to ARAMEMNON consensus prediction. 1. the comparison between the N-terminus of TROL and the N-terminal polypeptide microsequenced from the spinach AMS preparation. 2. the comparison between the C-terminus of TROL and the FNR-binding domain of the Tic62 vascular plants family. Sequences were retrieved from GenBank and plantGDB. The alignments were performed with ClustalW.

```

Transit peptide
MEALKTATPS FMSVLSEKRS EPRKPFSLPN LFPPKSQRPI SQESFLKRFN GGLALLTSVL 60
↓
SSATAPAKSL TYEEALQOSM TTSSSFDSGD LIEIGISNFVT TM helix
1. L TYEEALEQSV NADVGAEFDA DNPLVIAGGV AALAVPFVLS 120
QVLNKKPKSW GVESAKNAYT KLGTDNAQL LDIRATADFR QVGSFNKGL GKKA VSTVYN 180
Rhodanese-like domain
GEDKPGFLKK LSLKFKDPEN TTYIILDKFD GNSLVVAELV ALNGFKSAYA IKDGAEGPRG 240
TM helix
WLNSSLPWIE PKKTLSDLDS SLTDSISGVF GESSDGVSVV LGVAAAAGLS VFAFTEIETI 300
LQLLGSAAV QLAGKLLFA EDRKQTLKQV DEFINTKVAP KELVDELKEI GKALLPQSTS 360
PVP hinge
NKALPAPATV TAAEASATAT TTTVDKPVPE PETVAATTTT VDKPVPEPEP VPEPVVPAI 420
EAAVAAQVIT EPTETEAKPK PHSRPLSPYA SYPDLKPPSS PMPSPQ
2. ...SRRPLSPYA NYPDLKPPSS PTPSKP...T. aestivum
...----LSPFA AYPDLKPPSS PSPNAP...M. truncatula
...TEQPLSPYT AYDDLKPPSS PSPTKP...P. sativum
...AKQPLSPYI VYDDLKPPSS PSPSQP...G. max
...SQRPLSPYT AFVDLKPPSS PSPCPP...O. sativa
...AAAPLSPYT AYAEKPPPTS PSPIPP...L. esculentum
...KERPLSPYA RYENLKPPSS PSPTAS...A. thaliana
***: : :****: * *

```

construct was transiently expressed into isolated Arabidopsis protoplasts. The fusion protein clearly accumulated exclusively in chloroplasts, mainly associated with thylakoid membranes, visible as luminous foci (Figure 2a). *In organello* import into isolated chloroplasts was performed to further corroborate chloroplast localization and integration of the polypeptide into the thylakoid membranes. Following *in vitro* transcription/translation, the [³⁵S]-methionine labelled precursor of At4g01050 (Figures 3a,b, lane 1) was incubated with isolated intact chloroplasts. Labelled precursor was imported into organelles and processed into a smaller mature protein (Figure 3b, lane 3). The imported protein co-purified entirely with the thylakoid fraction (Figure 3b, indicated by an arrow). A weak signal similar in size with labelled precursor could also be detected (Figure 3b, indicated by an asterisk). This signal was protected from protease digestion (Figure 3a, indicated by an asterisk) and in all subsequent treatments behaved in an identical manner to the mature sized protein. The imported protein could not be extracted from the membranes by high salt, urea or high pH treatments (Figure 3b, lines 4–11). These experimental observations provide strong evidence that At4g01050 is an integral thylakoid membrane protein. Because of its obstinate interaction with thylakoid membranes and because of the presence of a well defined rhodanese-like homology domain, At4g01050 was consequently designated TROL, for thylakoid rhodanese-like protein.

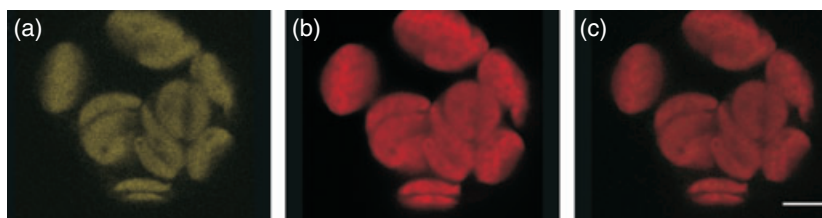
Digitonin solubilization and subsequent differential centrifugation to separate appressed and non-appressed

regions of thylakoid membranes were used to assess the lateral distribution of TROL in thylakoid membranes (Figure 3c). TROL is confined to a fraction which includes components of the PSI antenna (LHCI), cytochrome *f* and the majority of the thylakoid-bound FNR. In contrast, PSII core protein D1 and light-harvesting chlorophyll *a/b*-binding protein (LHCII) are enriched in the appressed region of the grana stacks. The β -subunit of ATP synthase was approximately equally distributed in both fractions. It can therefore be concluded that TROL has a heterogeneous lateral distribution and is mainly confined to the non-appressed regions of the thylakoid membrane system.

The presence of a protease-resistant band *in organello* import assays that corresponded in size with the [³⁵S]-methionine labelled precursor and that co-purified with the insoluble membrane fraction, prompted us to hypothesize that TROL might be present in a non-processed form at the chloroplast envelopes. To test this hypothesis, we isolated mixed outer and inner envelope vesicles and subjected them to immunochemical analysis using anti-TROL antibody. TROL antigenic activity was detected in the envelope vesicles in a protein band with an apparent molecular weight of 70 kDa (Figure 3d, lane 1). This size corresponded with the size of the labelled precursor, as tested by co-migration in different gel systems. TROL can thus be found in thylakoids, in its mature form and in envelopes, in its non-processed form. Moreover, the observed resistance to protease treatments in import experiments suggests that TROL is present at the inner envelope. Such heterogeneous

Figure 2. Subcellular localization of TROL-YFP. Confocal laser scanning microscope images of Arabidopsis protoplasts expressing TROL-YFP fusion (a–c).

(a) YFP fluorescence; (b) chlorophyll autofluorescence; (c) merged image. Scale bar = 6 μ m.



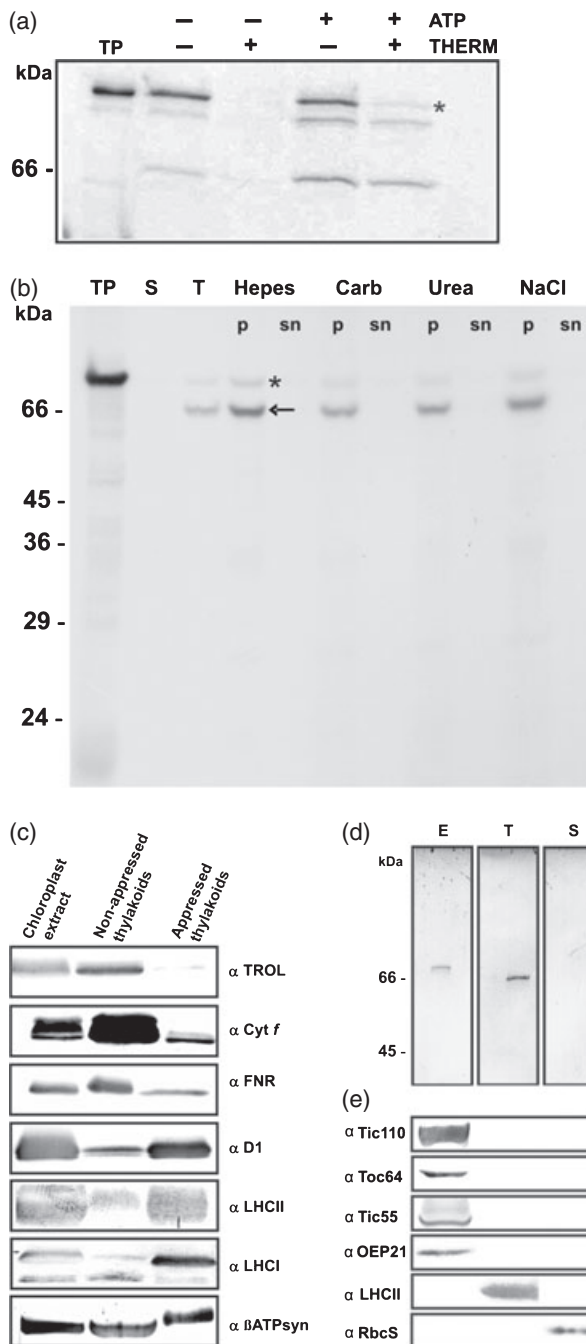


Figure 3. Subchloroplast localization and membrane association of TROL. (a) Low energy binding and protease protection assay. The TROL precursor obtained through *in vitro* transcription/translation (TP) was incubated with intact *Arabidopsis* chloroplasts for 17 min at 25°C in the dark. Import reactions were set up as indicated. Autoradiogram of 10% SDS-PAGE. Under low-energy conditions (extrinsic ATP not added) the radiolabelled precursor binds to the chloroplast envelope and disappears after thermolysin (THERM) digestion. In the presence of 3 mM ATP, precursor was imported into chloroplasts, which was further confirmed by protease treatment. Imported TROL precursor remains protected from protease digestion (asterisk). (b) TROL chloroplast import assay was performed under 50 $\mu\text{mol}_{\text{PHOTONS}} \text{m}^{-2} \text{s}^{-1}$ for 17 min at 25°C. Autoradiogram of 12.5% SDS-PAGE. Chloroplasts were subfractionated into stroma (S) and thylakoids (T). Radiolabelled TROL precursor (TP) was imported into organelles and processed into the mature sized protein (arrow). A weak signal similar in size to the labelled precursor was also detected (asterisk). The imported protein could not be extracted (supernatant, sn) from membranes (pellet, p) using 50 mM HEPES; 0.1 M Na_2CO_3 , pH 11 (Carb); 6 M urea; 4 M NaCl, respectively. (c) Lateral distribution. Thylakoids were subjected to digitonin solubilization and subsequent differential centrifugation to separate appressed and non-appressed regions. Protein samples (50 μg protein/lane) were analysed by immunoblotting using the indicated antibodies. (d) TROL is present at the chloroplast envelopes in a non-processed form. Chloroplast outer and inner envelope (E), thylakoids (T) and stroma (S) were loaded in equal amounts (10 μg protein/lane) and analysed by immunoblotting using anti-TROL antibody. (e) The purity of sample fractions in (d) was assessed by immunoblotting using indicated antibodies. The positions of molecular weight markers are indicated on the left.

distribution is unusual, but has also been identified for the At4g01050 in the proteome analysis of chloroplast envelopes and thylakoid membranes (Peltier *et al.*, 2004).

TROL interacts with FNR

The C-terminus of TROL contains a region of high sequence similarity to the Tic62 protein family interaction modules implicated in tethering the FNR flavoenzyme (Figure 1). Although the Tic62 protein FNR interacting modules are present in three imperfect repeat motifs, it has been

demonstrated that even one repeat module is sufficient to bind FNR (Küchler *et al.*, 2002). The module in TROL, designated ITEP (residues I429–P466), contains a highly conserved sequence KPPSSP (Figure 1, second alignment), which in other Tic62 protein family members is necessary for establishing high-affinity interaction with FNR flavoenzyme (Balsera *et al.*, 2007). In order to test whether the 38-residue domain of TROL is able to interact with FNR, we performed the yeast two-hybrid screen using the ITEP region as a bait and FNR as a target protein. In control experiments, two additional regions of TROL cDNA, which we assumed do not participate in establishing TROL–FNR interaction, were used as bait proteins. The two modules were designated 220 (residues N180–V220) and PEPE (residues A379–A419). The entire protein sequence was not used as TROL is a trans-membrane protein. Following transformation with 220 and PEPE into yeast cells, interaction with FNR was not detected (Figure 4a). As a positive control we used the IA2 sequence from the Tic62 protein (Küchler *et al.*, 2002). IA2 induces yeast growth in the presence of FNR as a target (Figure 4a). Vigorous growth of yeast cells carrying the FNR/ITEP combination provided a clear indication of a very strong interaction between the ITEP module and FNR (Figure 4a). In order to assess the difference in the strength and efficiency of the interaction between FNR and ITEP module of TROL versus FNR and IA2 module of Tic62, we performed photometric quantification of β -galactosidase activity for the positive combinations. To our surprise, the interaction between ITEP and FNR resulted in more than 8-fold stronger activation of β -galactosidase (Figure 4b). This result strongly

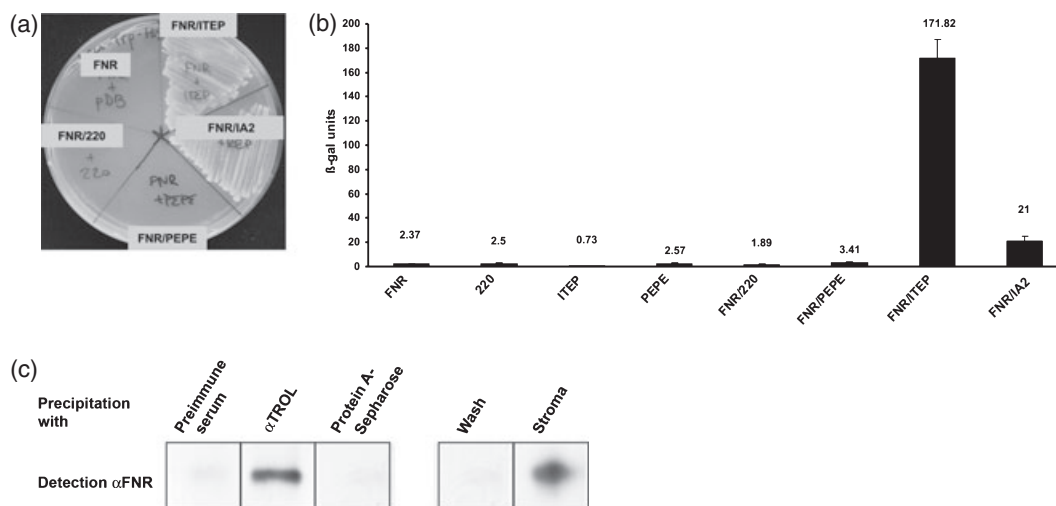


Figure 4. TROL strongly interacts with FNR.

(a) Qualitative yeast two-hybrid analysis. Growth of cells carrying the FNR/ITEP combination provided a clear indication of HIS3 reporter gene activation and a very strong interaction between ITEP module and FNR protein. Significant growth of cells carrying the FNR/IA2 combination indicated a strong interaction between Tic62 module and FNR protein, as expected. Protein-protein interactions were detected by yeast cells growth on SD medium lacking leucine, tryptophane and histidine. (b) Quantitative yeast two-hybrid analysis. Activation of β -galactosidase (*lacZ*) reporter gene in yeast cells carrying the indicated constructs was assessed by photometric quantification. Values are means of triplicate measurements with error bars representing standard deviation. The experiment was repeated twice with similar results.

(c) Coimmunoprecipitation of FNR with TROL. Protein samples were analysed by immunoblotting using anti-FNR antibody. FNR was highly detectable in the immunoprecipitated fraction (α TROL) comparing with the negative controls (pre-immune serum; Protein A-Sepharose; Protein A-Sepharose wash).

indicates that the ITEP repeat from TROL serves as a much better interaction module than IA2. The presence of a bulky methionine residue at position 462 of TROL (Figure 1, second alignment) might alleviate the interaction between ITEP and FNR.

In a second approach, thylakoid membranes were solubilised with 1% Triton X-100 and TROL antibodies were used for immunoprecipitation (Figure 4c). FNR was strongly enriched in the immunoprecipitated fraction (Figure 4c, α TROL) in comparison with the pre-immune serum which was used in a control experiment. Also, no detectable amounts of FNR were present in the lane containing a fraction incubated with Protein A-Sepharose alone. These data strongly indicate that FNR is affiliated with TROL *in planta*.

TROL-deficient mutants have distinct leaf anatomy and chloroplast size

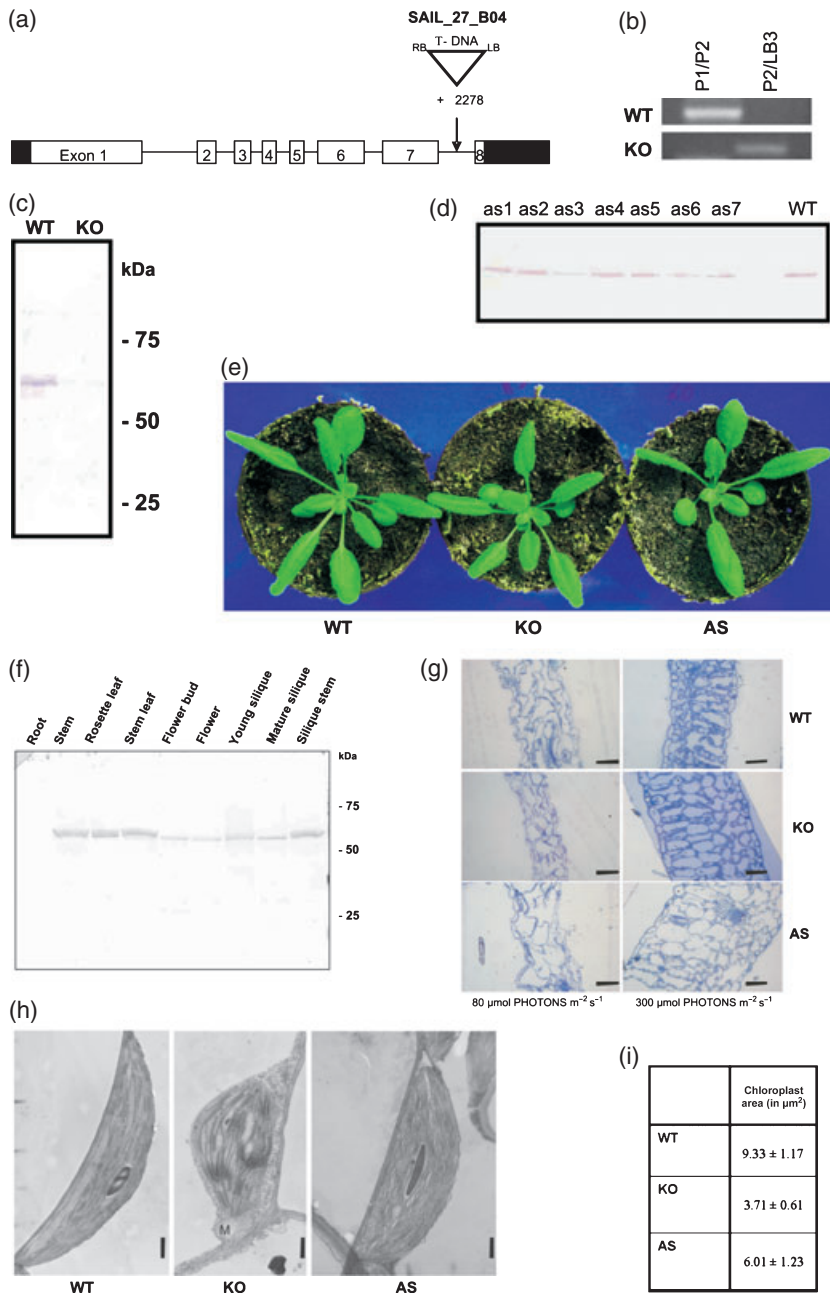
To gain further insight into the *in vivo* function of TROL, we subsequently analysed a T-DNA mutagenized line of the Arabidopsis plants. The SAIL_27_B04 mutant line contained a single T-DNA element inserted into the last intron of At4g01050 at position 2278 (Figure 5a). Plants selected for the homozygous presence of the T-DNA insertion in the At4g01050 locus (Figure 5b) were further analysed using antibodies against TROL (Figure 5c). Only plants with a complete absence of TROL (knock-out plants) were taken for further analyses. The phenotype of knock-out plants did not significantly differ from the wild type (Figure 5e), although

knock-out plants were a bit slower in development and produced smaller rosettes. Frequently, their inflorescence appeared yellowish with siliques being particularly affected. In the wild-type the accumulation of TROL was the lowest in those organs (Figure 5f).

We further investigated the content of photosynthetic pigments in the wild-type and the mutant plants. The knock-out plants had slightly, but not significantly, increased chlorophyll *a* and carotenoids content, whereas the Ca + Cb/Car ratio was reduced to 5.7 (Table S1). An increased amount of carotenoids has been shown to have a photoprotective role (Lichtenthaler, 2007).

Semi thin transversal sections were made in order to investigate the anatomy of mutant leaves. Leaves from plants grown in a growth-light regime ($80 \mu\text{mol}_{\text{PHOTONS}} \text{m}^{-2} \text{s}^{-1}$ of white light) had large mesophyll cells with irregular shapes (Figure 5g). In mutant plants, cells appeared even larger and with more intercellular spaces. When grown in a high-light regime ($300 \mu\text{mol}_{\text{PHOTONS}} \text{m}^{-2} \text{s}^{-1}$ of white light), the leaf structure appeared unaltered, with palisade and spongy parenchyma having regular morphology (Figure 5g). Interestingly, the thickness of the mutant leaves was enlarged. This might be the result of a general stress response, or may reflect the connection between the physiological states of the photosynthetic machinery with the leaf morphology. A similar effect was observed in *immutans* plants (Rodermeil, 2001).

To gain further insight into the mutant phenotype, we investigated the ultrastructure of mutant and wild-type



plants by using electron microscopy (Figure 5h). The ultrastructure revealed about twice as many smaller chloroplasts with irregular morphology in knock-out as in wild-type plants (Figure 5h). These smaller chloroplasts contained no starch grains and resembled plastids found in younger tissues. Photosynthetic membranes were not abundant and they appeared to have more non-appressed regions. In every case, envelope membranes were continuous and seemed normally developed. Mitochondria appeared to be unaffected by the mutation in size and fine structure.

To further substantiate these findings, we created transgenic Arabidopsis plants harbouring an antisense construct of At4g01050 (Figure 5d). In using this approach, our aim was to verify the results obtained analysing the knock-out plants, in which the T-DNA insertion may lead to undesired genome rearrangements. Light and electron microscopy of leaf sections revealed leaf anatomy, structures and plastids with comparable phenotypic characteristics as observed in the wild-type (Figure 5h). The photosynthetic pigment composition was not significantly different from the wild-type (Table S1). When plants were grown in a high-light

Figure 5. TROL-deficient plants show altered leaf anatomy and ultrastructure.

(a) Schematic representation of the T-DNA insertion in At4g01050. The exact site of the T-DNA insertion was determined by sequencing. Black boxes represent 5' untranslated region and 3' untranslated region, respectively.

(b) The PCR analyses of plants homozygous for the T-DNA insertion. Primers P1 and P2 were used to amplify the 'wild-type' sequence, present in WT and heterozygous plants, and primers P2 and LB3 were used to amplify the 'transgene' sequence, consisted of gene fragment and T-DNA left border fragment. Only plants with 'transgene' sequence amplified were used in further experiments.

(c) The Western Blot analyses. Total protein extracts were loaded in equal amounts (80 µg protein/lane) and immunoblotted with anti-TROL antibody. The positions of molecular weight markers are indicated on the right.

(d) The identification of antisense plants with decreased amount of TROL. The plant as3 progeny was used in further experiments. Total protein extracts were loaded in equal amounts (80 µg protein/lane) and immunoblotted with anti-TROL antibody.

(e) Phenotype of mutant plants compared with the wild type. Knock-out line (KO) and antisense line (AS) did not significantly differ from the wild-type (WT) under growth-light conditions.

(f) TROL accumulates in a tissue-specific manner. Protein extracts from indicated plant tissues were isolated from 6- to 7-week-old wild-type Arabidopsis plant, loaded in equal amounts (100 µg protein/lane), and immunoblotted with anti-TROL antibody. The positions of molecular weight markers are indicated on the right.

(g) Leaf anatomy of plants grown under growth-light (left panels) and under high-light (right panels). Scale bar = 100 µm.

(h) Chloroplast ultrastructure of plants grown under growth-light conditions. Scale bar = 1 µm.

(i) The surface of chloroplasts. Data are represented as mean ± SEM.

regime, the thickness of the antisense leaves was larger than in the wild-type and in the knock-out line. Also, the surface of chloroplasts was about $6 \mu\text{m}^2$. (Figure 5i).

TROL depletion impairs LEF

In order to test how TROL inactivation influences photosynthetic electron flow we have subjected wild-type, knock-out and antisense lines to measurements of *in situ* chlorophyll fluorescence. We measured the photosynthetic performance of wild-type, knock-out and antisense leaves by pulse amplitude fluorometry (PAM). Values of maximum quantum yield of PSII (Fv/Fm) were 0.82 in all sample types, indicating that wild-type plants as well as transgenic lines had fully functional PSII. The PSII driven electron transport rate (rel. ETR) was also similar at lower irradiances (Figure 6a). However, at higher light intensities (500 and $800 \mu\text{mol}_{\text{PHOTONS}} \text{m}^{-2} \text{s}^{-1}$) rel. ETR values were severely lowered in knock-out and antisense lines with respect to wild-type plants (Figure 6a). Simultaneously, the NPQ at higher light intensities increases in the transgenic lines, indicating enhanced dissipation of absorbed light energy as heat (Figure 6b). Thus, TROL-deficient thylakoids direct a smaller fraction of absorbed light to the electron transport chain than thylakoids of the wild-type plants.

We further addressed the question of the involvement of TROL in CEF around PSI. The rate of cyclic flow was measured in dark-adapted leaves under aerobic conditions submitted to a saturating illumination. CEF was measured as P700 redox kinetics in intact leaves with a flash spectrophotometer as described (Nandha *et al.*, 2007). P700 oxidation was measured at 820 nm (Breyton *et al.*, 2006), upon specific excitation by far-red illumination. CEF was then quantified by assessing the rate of PSI turnover under conditions where PSII activity was largely prevented (because of illumination with far-red light Breyton *et al.*, 2006). In dark-adapted leaves, very slow oxidation of P700 resulted from multiple PSI turnovers, due to cyclic flow. In contrast, very fast

oxidation in light-adapted leaves was due to linear flow, where PSII activity could not support enhanced PSI turnover. By this test, we estimated that almost 100% of PSI could be involved in CEF in the dark, while this process did not involve more than 10–20% of this complex in the light-acclimated conditions. We observed no differences in CEF rates in TROL-deficient plants (P. Joliot, G. Finazzi, H. Fulgosi, Institut de Biologie Physico-Chimique, Paris, France, unpublished data). To further substantiate these findings, we investigated changes in chlorophyll fluorescence traces as measured by their transient increase due to CEF (Munekage *et al.*, 2004). In every case, we observed an increase in chlorophyll fluorescence after turning off actinic light (Figure S2b, boxed area). However, this method analyses only the NADPH dehydrogenase-dependent CEF. Main cyclic flow mediated by ferredoxin-quinone oxidoreductase could not be evaluated with this method.

As the absence of TROL might lead to overreduction of the photosynthetic machinery, we further analysed possible changes in state 1–state 2 transitions. In low-light, no changes could be observed (Figure S2a,b). In the light conditions of $500 \mu\text{mol}_{\text{PHOTONS}} \text{m}^{-2} \text{s}^{-1}$, variable chlorophyll fluorescence was strongly quenched in TROL-deficient plants (Figure S2b). Apparently, the absence of TROL contributes to an increased ability of photosynthetic membranes to dissipate excess energy. It is possible that this effect is also linked to FNR solubilization.

To analyse how much FNR is still bound to photosynthetic membranes when TROL is not present, we subjected isolated and salt-washed thylakoids from the wild-type and knock-out plants to immunochemical analysis using anti-FNR antibodies. Thylakoids from the knock-out plants contained detectable, but greatly reduced amounts of FNR as compared with the wild-type (Figure 7a). TROL deficiency has generally not lowered the amount of FNR in chloroplasts, as judged from the control immunoblots (Figure 7b). Furthermore, accumulation of TROL and FNR on the

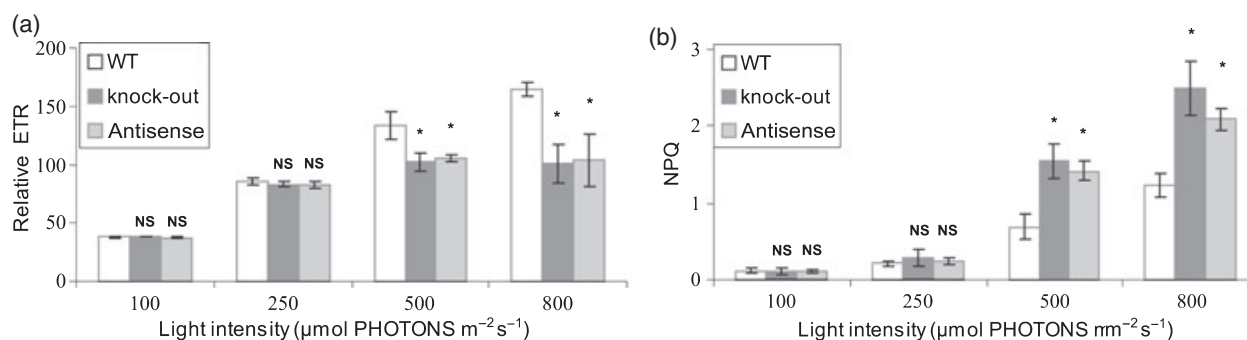


Figure 6. TROL-deficient plants are impaired in LEF.

(a) Light-intensity dependence of relative ETR. At higher light intensities ETR values were severely lowered in knock-out and antisense lines with respect to wild-type plants. Values are means of five independent measurements with error bars representing standard deviation. Data were statistically evaluated using *t*-test for the small sample, **P*(*t*) <1%. NS, non-significant difference.

(b) Light-intensity dependence of NPQ. Values are means of five independent measurements with error bars representing standard deviation. Data were statistically evaluated using *t*-test for the small sample, **P*(*t*) <1%. NS, non-significant difference.

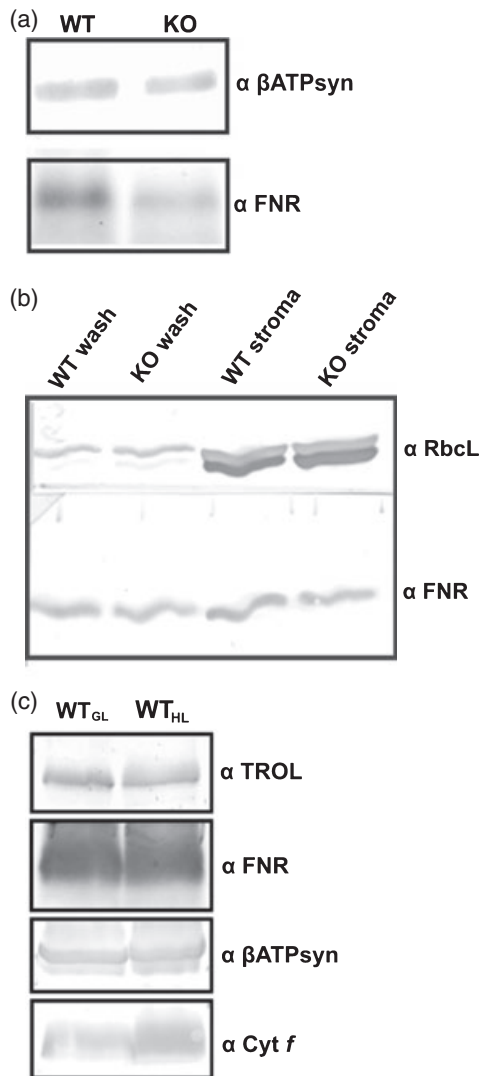


Figure 7. TROL-deficient thylakoids bind significantly less FNR. (a) Thylakoids were isolated from wild-type (WT) and knock-out (KO) plants growing under growth-light conditions as described in Supporting information, and washed with 0.5 M NaCl. Extracts were loaded in equal amounts (10 µg protein/lane), and immunoblotted with anti-FNR antibody. (b) The supernatant after extraction of thylakoids with 0.5 M NaCl (Wash) and the stroma extracts were immunoblotted with the indicated antibodies to show the soluble fraction of FNR. (c) Thylakoids were isolated from wild-type plants growing under growth-light (WT_{GL}) and high-light (WT_{HL}) conditions as in (a). Extracts were loaded in equal amounts (15 µg protein/lane), and immunoblotted with the indicated antibodies.

thylakoid membranes was assessed under conditions of high-light and no changes were observed (Figure 7c).

Multiprotein complexes containing TROL

The relationship between TROL and other thylakoid protein complexes, in particular cytochrome *b₆/f*, PSI and PSII, was studied using blue-native polyacrilamide gel electrophoresis (BN-PAGE); (Figure 8). In TROL-deficient mutant, the accu-

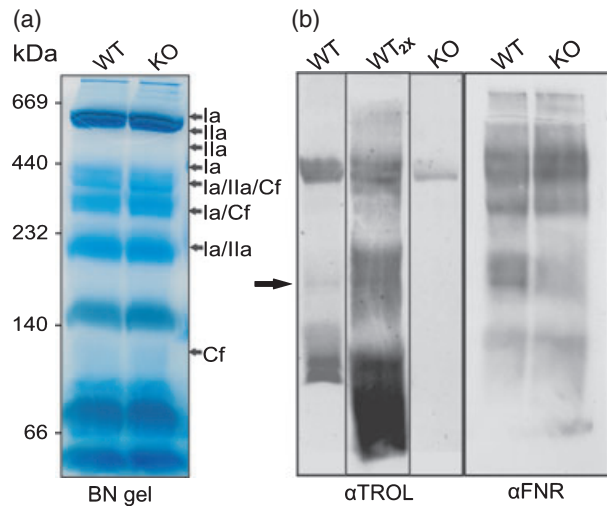


Figure 8. BN-PAGE of thylakoid protein complexes containing TROL and FNR.

(a) Thylakoid membranes (50 µg of chlorophyll) were solubilised with 1.23% dodecyl- β -D-maltoside and separated by 4–12% native gel. Positions of thylakoid proteins identified with specific antibodies are indicated: Ia, PSI-A; IIa, D1; Cf, Cyt *f*. The positions of HMW native markers are indicated on the left. (b) Thylakoid membrane complexes separated by BN-PAGE in (a) were further subjected to immunoblotting with antibodies against TROL and FNR. Arrow indicates the position of the TROL–FNR complex in WT at about 190 kDa, but completely missing in KO. TROL could also be found at 110, 120, and 420 kDa. Undetermined immunoreactive band at 420 kDa in KO lane was detected. WT_{2x}, 100 µg of chlorophyll loaded in the well.

mulation and stability of the major thylakoid multiprotein complexes were not noticeably affected (Figure 8a). Immunoblot analyses indicated that TROL could be found in the three major complexes, at 110, 120 and 420 kDa. The 420 kDa complex might contain representative subunits of cytochrome *b₆/f*, PSI and PSII. TROL associated with FNR could be found in probably transient complex at about 190 kDa (Figure 8b, indicated by an arrow). Loss of FNR binding to TROL depleted thylakoids is substantial in the 190 kDa range (Figure 8b, KO lane). FNR was found to be associated with a number of other protein complexes (Figure 8b), suggesting that TROL is an important, but not exclusive site for FNR association with thylakoid membranes.

Depletion of TROL modulates the expression of a specific set of nuclear-encoded genes

The observed anatomical and ultrastructural changes in TROL-deficient plants prompted us to investigate changes in global gene expression patterns. A total number of 237 differentially expressed genes were selected according to *q*-value <0.001 cut-off (Table S3). To demonstrate the biological meaning of the observed changes, from this set of genes those encoding chloroplast-targeted proteins were further selected (Table S2). Among up-regulated genes are POR B, which uses NADPH for chlorophyll biosynthesis and the NADP–malic enzyme, which potentially generates

NADPH in an alternative pathway. It is possible that TROL deficiency negatively influences NADPH synthesis, which plants try to compensate by redirecting the NADPH synthesis pathway from FNR to the NADP-malic enzyme. Furthermore, modulation of genes involved in biosynthesis and trafficking of tocopherol, as well as, DNAJ protein, thioredoxin and glutathione-S-transferase indicates that TROL-deficient plants might use metabolic retrograde signalling to adapt their responses to oxidative stress. Interestingly, the expression of several envelope membrane protein transcripts (At1g07420, At2g19450, At5g62720, At2g28900, At1g10760, At1g23740, At5g64940) is also altered, possibly connected with TROL function at the inner envelope.

DISCUSSION

In this report, we characterized a protein that is required for anchoring the FNR flavoenzyme to the thylakoid membranes and sustaining high efficiency photosynthetic LEF.

FNR is an enzyme that has to combine the interaction with a bulky proteinaceous Fd with electron transfer to a relatively small, easily diffusible, NADP⁺ molecule. This reaction has to be fast and efficient to enable high rates of photosynthesis and to prevent over-reduction of the entire thylakoid electron transfer chain. In order to enable efficient electron transfer, electron donor and acceptor have to be positioned in an optimal orientation with respect to their redox centres. The absence of TROL disables FNR from being tethered to the membrane, therefore a substantial amount of FNR remains soluble. Forti and Bracale (1984) demonstrated that the soluble form of FNR is very inefficient in NADP⁺ photoreduction by isolated thylakoids. In our case, linear photosynthetic flow can be sustained until light intensity exceeds 250 $\mu\text{mol}_{\text{PHOTONS}} \text{m}^{-2} \text{s}^{-1}$. As soluble FNR is no longer able to reduce NADP⁺ at high rates, this could lead to over-reduction of the entire electron transport chain. In this case, NPQ modulation could be particularly important to prevent photo-damage caused by build-up of reduced electron carriers which block LEF before the lumen could be significantly acidified (Kanazawa and Kramer, 2002). Overexpression of FNR in transgenic plants causes enhanced tolerance to photo-oxidative damage and herbicides that propagate reactive oxygen species (Rodriguez *et al.*, 2007). On the other hand, antisense repression of FNR renders transgenic plants abnormally prone to photo-oxidative injury (Palatnik *et al.*, 2003). If solubilization of FNR is necessary for the regulation of oxidative stress, then it is not surprising that, under high-light conditions, TROL-deficient plants exhibit increased rates of NPQ. This effect could also be attributed to recently proposed feedback redox regulation *via* the redox poise of the NADP(H) pool (Hald *et al.*, 2008). Inhibition of TROL accumulation by antisense expression results in quenching which is higher than that of the wild-type plants, but lower than that of the TROL knock-out plants (Figure 6d). This demonstrates dosage effect of TROL

and indicates that FNR binding to the thylakoid membranes is dependent on the availability of tethering sites and that the amount of soluble FNR directly influences NPQ.

TROL is confined to non-appressed regions of thylakoid membranes, most likely not associated with any major photosynthetic complexes. Localization in non-appressed regions places TROL in the vicinity of the site of Fd reduction. The results shown in Figure 8(b) may indicate the presence of several TROL subpools in the thylakoid membrane. It appears that only 190 kDa complex contains TROL in association with the FNR. The amount of FNR bound to this complex is substantial and favours the important role of TROL-FNR association in maintaining efficient LEF. Complexes at about 110 and 120 kDa indicate the existence of a small ligand which may be associated with other TROL domains, namely the large rhodanese-like domain which is predicted to be located in the thylakoid lumen. Apart from being involved in sulfur metabolism, rhodanese-like domains are implicated in redox regulation of various intracellular processes (Horowitz and Falksen, 1986; Horowitz *et al.*, 1992; Nandi *et al.*, 2000). In fact, progression of the eukaryotic cell cycle, controlled by Cdc25 phosphatases, appears to be regulated via intracellular redox change (see Rudolph, 2005; and refs. therein). It is tempting to speculate that the rhodanese-like domain of TROL is involved in redox regulation of FNR binding and release. It is possible that the rhodanese-like domain interacts directly with plastoquinone. The NMR structure of TROL rhodanese-like domain reveals a slightly altered loop (Pantoja-Uceda *et al.*, 2005) which might accommodate the plastoquinone molecule. In Cdc25 phosphatases, quinone binding to an active rhodanese domain is responsible for modulation of phosphatase activity (Brisson *et al.*, 2005). It appears that irreversible oxidation of the active-site cysteine is a mechanism by which quinones inactivate the phosphatase (Garuti *et al.*, 2008). In TROL, redox regulation of FNR binding and release could be important for balancing the redox status of stroma with the membrane electron transfer chain. Such regulation could be important for prevention of over-reduction of any of these two compartments and maintenance of the redox poise.

Localization of the TROL precursor in the chloroplast envelope indicates its possible role in electron transfer chain specific for this membrane. Additional FNR binding to the inner envelope takes place *via* Tic62 (Küchler *et al.*, 2002). It has been proposed that this type of binding is required for redox regulation of pre-protein import across the inner envelope (Küchler *et al.*, 2002). TROL is present at the inner envelopes in its unprocessed form. This dual localization might also be dependent on the NADP⁺/NADPH ratio in the chloroplasts, similar to the shuttling of the Tic62 protein (Stengel *et al.*, 2008).

TROL inactivation modulates the expression of 237 nuclear genes, revealing a novel retrograde signaling pathway. Chloroplasts are the major source of NADPH

which is exported to the cytosol where it participates in various redox-dependent processes. TROL-deficient plants appear to try to compensate the deficiency in NADPH production by up-regulating the gene for malic enzyme which can potentially generate NADPH in an alternative pathway. Also, genes encoding proteins involved in stress management are strongly up-regulated. As plant growth and development are driven by electron transfer reactions (Noctor, 2006), it is not surprising that leaf anatomy is altered in the knock-out. Furthermore, chloroplasts in the knock-out are small and have less developed thylakoids. These morphological changes reflect alterations in gene expression of a specific set of genes encoding chloroplast proteins (Table S2). Many processes important for chloroplast morphogenesis could be influenced by NADPH production, or be dependent on metabolic retrograde signaling.

In conclusion, TROL represents a long-sought component of photosynthetic membranes responsible for docking of the flavoenzyme FNR. This interaction appears to be important for maintenance of efficient LEF, induction of NPQ and metabolic retrograde signaling. Furthermore, discovery of TROL provides new information for linking leaf and chloroplast morphogenesis with photosynthetic cues.

EXPERIMENTAL PROCEDURES

Plant material and growth conditions

Arabidopsis thaliana (L.) ecotype Columbia (Col-0) plants and mutant lines were grown on soil at 20°C under 80 $\mu\text{mol}_{\text{PHOTONS}} \text{m}^{-2} \text{s}^{-1}$ (growth-light), a 16-h photoperiod and a relative air humidity of 60% (day) and 70% (night). For leaf anatomy and leaf ultrastructure plants were grown under growth-light and 300 $\mu\text{mol}_{\text{PHOTONS}} \text{m}^{-2} \text{s}^{-1}$ (high-light), respectively. For electron transport analysis plants were grown under 300 $\mu\text{mol}_{\text{PHOTONS}} \text{m}^{-2} \text{s}^{-1}$. The T-DNA insertion line in the Columbia background for At4g01050 (SAIL_27_B04) was obtained from NASC (Scholl *et al.*, 2000).

Import assay

pZL1 plasmid containing the full-length cDNA clone of At4g01050, obtained from ABRC stock centre (accession number 109P22), was linearized with *Xba*I immediately downstream of the insert. Import was done according to Fulgosi *et al.* (1998). For the protease protection assay import reactions were treated with thermolysin (end conc. 100 $\mu\text{g} \text{ml}^{-1}$) for 20 min. Reaction was stopped by addition of 5 μl 0.5 M EDTA, pH 8.0. To monitor for possible membrane association of TROL, thylakoids were incubated on ice in the presence of the reagents indicated in Figure 3(b).

Immunoprecipitation assay

Thylakoids were resuspended in buffer containing 20 mM HEPES, pH 7.5; 15 mM NaCl; 5 mM MgCl_2 . The thylakoid membranes were incubated with Triton X-100 at 0°C for 30 min. The Triton/Chl (w/w) ratio was adjusted to 25:1. After centrifugation at 40 000 g for 30 min, the supernatant was incubated with either anti-TROL antibody or pre-immune serum at 4°C overnight. The antibody complexes were precipitated using Protein A-Sepharose (Amersham Pharmacia Biotech, <http://www5.gelifesciences.com>). Proteins

released after boiling of resin were separated by SDS-PAGE and immunoblotted with anti-FNR antibody. Signals were visualized with ECL.

Yeast two-hybrid assay

Three cDNA fragments encoding N180-V220 (220), A379-A419 (PEPE) and I429-P466 (ITEP) of TROL protein were fused to Gal4 DNA binding domain in the pBD-Gal4 vector (Stratagene, <http://www.stratagene.com>). IA2 sequence from Tic62 protein, spanning the region from amino acid residues 263 to 444, in pBD-Gal4 vector was used as a positive control and the full length cDNA of psFNR (accession number X12446), fused to Gal4 activation domain in the pAD-Gal4-2.1 plasmid (gifts from Dr J. Soll) was used as a target. After the successful cloning was confirmed by sequencing, all the plasmids and their combinations were transformed using LiAc method in to the yeast strain. *S. cerevisiae* YF53 (Mata ura3-52 his3-200 ade2-101 lys2-801 trp1-901 leu2-3,112 gal4-542 gal80-538, with HIS3 and *lacZ* reporter gene constructs LYS2::UASGAL1-TAGAL1-HIS3 and URA3::UASGAL4 17 mers ($\times 3$)-TATACYC1-*lacZ*) was used. Transformants were selected on SD medium without leucine and tryptophane and protein-protein interactions were detected by growth on SD medium lacking leucine, tryptophane and histidine and by the β -galactosidase assay. Specific β -galactosidase activities were determined from yeast cultures by the method of Adams *et al.* (1997). All assays were performed in duplicate from at least three independent colonies in 0.5 ml of reaction buffer and β -galactosidase units were calculated as described (Feilolter *et al.*, 1994).

Blue-native PAGE

Intact Arabidopsis chloroplasts, isolated as described in Supporting information, were sedimented by centrifugation at 1000 g for 10 min. Sediment equivalent to 50 μg of chlorophyll were ruptured in lysis buffer pH 6.8 (10 mM Tris/HCl; 10 mM MgCl_2 ; 20 mM KCl) and sedimented by centrifugation at 1000 g for 2 min. The sediment was solubilized in solubilization buffer (750 mM 6-aminohexanoic acid; 50 mM Bis-Tris, pH 7.0; 0.5 mM EDTA, pH 7.0; 1.23% dodecyl- β -D-maltoside) for 30 min on ice in the dark and then centrifuged at 21 000 g for 10 min. The supernatant was supplemented with 5 μl of a Coomassie-blue solution (5% (w/v) Coomassie-G; 750 mM 6-aminohexanoic acid) and loaded directly onto the gel. Gels consisted of a separating gel (gradient of 6–12% acrylamide) and a stacking gel (4% acrylamide). Gel composition and solutions for electrophoresis were prepared as described in Schägger *et al.* (1994). High molecular weight (HMW) native marker kit was purchased from GE Healthcare (<http://www5.gelifesciences.com>). The electrophoresis was carried out at 4°C, starting at 150 V for 45 min and continuing at 600 V (approximately 15 mA) for 2–3 h. After removal of excess dye, blue native gels were electroblotted onto nitrocellulose membranes at 4°C and 400 mA for 4 h. Membranes were probed with antibodies specific for individual thylakoid proteins and signals were detected with ECL.

Electron transport analysis

Chlorophyll fluorescence parameters were measured using a MINI-PAM portable chlorophyll fluorometer (Walz, <http://www.walz.com>). PSII driven rel. ETR and NPQ were calculated as $\text{PPFD} \times 0.5 \times \Phi\text{PSII}$ and $(\text{Fm} - \text{Fm}')/\text{Fm}'$, respectively, where PPFD is photosynthetic photon flux density, ΦPSII was calculated using the following expression: $(\text{Fm}' - \text{Fs})/\text{Fm}'$, Fm is maximum fluorescence level in dark-adapted material, Fm' is a maximum fluorescence level in the light and Fs is the steady-state fluorescence level.

ACKNOWLEDGEMENTS

We thank I. Adamska and A. Sokolenko for the kind gift of antibodies and M. Sopta for critical reading of the manuscript. We thank K. Philippar for the Affymetrix full genome microarray screen. This work was supported by the scientific research grant 098–0982913–2838 to H.F., research grant 073–0731674–1673 to H.L. and Technological Research and Development Grant E34/2006, all funded by the Croatian Ministry of Science, Education and Sports. The funding by the VW-foundation and the DFG (SFB-TR01/C7) to E.S. is acknowledged.

SUPPORTING INFORMATION

Additional Supporting Information may be found in the online version of this article:

Figure S1. Electrophoresis of subthylakoidal fractions.

Figure S2. State 1–state 2 transitions measurements.

Table S1. The content of photosynthetic pigments in wild-type and mutant plants.

Table S2. Selected significantly affected genes encoding chloroplast-localized proteins.

Table S3. Annotated list of genes significantly differentially expressed in TROL-deficient plants.

Experimental procedures S1.

References S1.

Please note: Wiley-Blackwell are not responsible for the content or functionality of any supporting materials supplied by the authors. Any queries (other than missing material) should be directed to the corresponding author for the article.

REFERENCES

- Adams, A., Gottschling, D.E., Kaiser, C.A. and Stearns, T. (1997) *Methods in Yeast Genetics: A Laboratory Course Manual*. USA: Cold Spring Harbor: Cold Spring Harbor Laboratory Press.
- Allen, J.F. (2002) Photosynthesis of ATP-electrons, proton pumps, rotors, and poise. *Cell*, **110**, 273–276.
- Allen, J.F. (2003) Cyclic, pseudocyclic and noncyclic photophosphorylation: new links in the chain. *Trends Plant Sci.* **8**, 15–19.
- Andersen, B., Scheller, H.V. and Moller, B.L. (1992) The PSI E subunit of photosystem I binds ferredoxin:NADP⁺ oxidoreductase. *FEBS Lett.* **311**, 169–173.
- Azumi, Y. and Watanabe, A. (1991) Evidence for a senescence-associated gene induced by darkness. *Plant Physiol.* **95**, 577–583.
- Balsera, M., Stengel, A., Soll, J. and Bötlér, B. (2007) Tic62: a protein family from metabolism to protein translocation. *BMC Evol. Biol.* **7**, 43.
- Bauer, M., Dietrich, C., Nowak, K., Sierralta, W.D. and Papenbrock, J. (2004) Intracellular localization of *Arabidopsis* sulfurtransferases. *Plant Physiol.* **135**, 916–926.
- Bordo, D. and Bork, P. (2002) The rhodanese/Cdc25 phosphatase superfamily. Sequence–structure–function relations. *EMBO Rep.* **3**, 741–746.
- Breyton, C., Nandha, B., Johnson, G.N., Joliot, P. and Finazzi, G. (2006) Redox modulation of cyclic electron flow around photosystem I in C3 plants. *Biochemistry*, **45**, 13465–13475.
- Brisson, M., Nguyen, T., Wipf, P., Joo, B., Day, B.W., Skoko, J.S., Schreiber, E.M., Foster, C., Bansal, P. and Lazo, J.S. (2005) Redox regulation of Cdc25B by cell-active quinolinediones. *Mol. Pharmacol.* **68**, 1810–1820.
- Caplan, J.L., Mamillapalli, P., Burch-Smith, T.M., Czymbek, K. and Dinesh-Kumar, S.P. (2008) Chloroplastic protein NR1P1 mediates innate immune receptor recognition of a viral effector. *Cell*, **132**, 449–462.
- Carrillo, N. and Ceccarelli, E.A. (2003) Open questions in ferredoxin–NADP⁺ reductase catalytic mechanism. *Eur. J. Biochem.* **270**, 1900–1915.
- Clark, R.D., Hawkesford, M.J., Coughlan, S.J., Bennett, J. and Hind, G. (1984) Association of ferredoxin–NADP⁺ oxidoreductase with the chloroplast cytochrome *b-f* complex. *FEBS Lett.* **174**, 137–142.
- Feilolter, H.E., Hannon, G.J., Ruddell, C.J. and Beach, D. (1994) Construction of an improved host strain for two hybrid screening. *Nucleic Acids Res.* **22**, 1502–1503.
- Forti, G. and Bracale, M. (1984) Ferredoxin–ferredoxin NADP reductase interaction. *FEBS Lett.* **166**, 81–84.
- Fulgosi, H., Vener, A.V., Altschmied, L., Herrmann, R.G. and Andersson, B. (1998) A novel multi-functional chloroplast protein: identification of a 40 kDa immunophilin-like protein located in the thylakoid lumen. *EMBO J.* **17**, 1577–1587.
- Garuti, L., Roberti, M. and Pizzirani, D. (2008) Synthetic small molecule Cdc25 phosphatases inhibitors. *Curr. Med. Chem.* **15**, 573–580.
- Hajirezaei, M.R., Peisker, M., Tschiersch, H., Palatnik, J.F., Valle, E.M., Carrillo, N. and Sonnewald, U. (2002) Small changes in the activity of chloroplastic NADP⁺-dependent ferredoxin oxidoreductase lead to impaired plant growth and restrict photosynthetic activity of transgenic tobacco plants. *Plant J.* **29**, 281–293.
- Hald, S., Nandha, B., Gallois, P. and Johnson, G.N. (2008) Feedback regulation of photosynthetic electron transport by NADP(H) redox poise. *Biochim. Biophys. Acta*, **1777**, 433–440.
- Hanke, G.T., Okutani, S., Satomi, Y., Takao, T., Suzuki, A. and Hase, T. (2005) Multiple iso-proteins of FNR in *Arabidopsis*: evidence for different contributions to chloroplast function and nitrogen assimilation. *Plant Cell Environ.* **28**, 1146–1157.
- von Heijne, G., Steppuhn, J. and Herrmann, R.G. (1989) Domain structure of mitochondrial and chloroplast targeting peptides. *Eur. J. Biochem.* **180**, 535–545.
- Horowitz, P.M. and Falksen, K. (1986) Oxidative inactivation of the enzyme rhodanese by reduced nicotinamide adenine dinucleotide. *J. Biol. Chem.* **261**, 16953–16956.
- Horowitz, P.M., Butler, M. and McClure, G.D. Jr (1992) Reducing sugars can induce the oxidative inactivation of rhodanese. *J. Biol. Chem.* **267**, 23596–23600.
- Kanazawa, A. and Kramer, D.M. (2002) *In vivo* modulation of nonphotochemical exciton quenching (NPQ) by regulation of the chloroplast ATP synthase. *Proc. Natl Acad. Sci. USA*, **99**, 12789–12794.
- Küchler, M., Decker, S., Hörmann, F., Soll, J. and Heins, L. (2002) Protein import into chloroplasts involves redox-regulated proteins. *EMBO J.* **21**, 6136–6145.
- Lichtenthaler, H.K. (2007) Biosynthesis, accumulation and emission of carotenoids, alpha-tocopherol, plastoquinone, and isoprene in leaves under high photosynthetic irradiance. *Photosyn. Res.* **92**, 163–179.
- Lintala, M., Allahvrdiyeva, Y., Kindon, H., Piippo, M., Battchikova, N., Suorsa, M., Rintamäki, E., Salminen, T.A., Eva-Mari, A. and Mulo, P. (2007) Structural and functional characterization of ferredoxin–NADP⁺-oxidoreductase using knock-out mutants of *Arabidopsis*. *Plant J.* **49**, 1041–1052.
- Medina, M. and Gómez-Moreno, C. (2004) Interaction of ferredoxin–NADP⁺ reductase with its substrates: optimal interaction for efficient electron transfer. *Photosyn. Res.* **79**, 113–131.
- Mintel, R. and Westley, J. (1966) The rhodanese reaction. Mechanism of thioisulfate binding. *J. Biol. Chem.* **241**, 3381–3385.
- Munekage, Y., Hashimoto, M., Miyake, C., Tomizawa, K.I., Endo, T., Tasaka, M. and Shikanai, T. (2004) Cyclic electron flow around photosystem I is essential for photosynthesis. *Nature*, **429**, 579–582.
- Nandha, B., Finazzi, G., Joliot, P., Hald, S. and Johnson, G.N. (2007) The role of PGR5 in the redox poising of photosynthetic electron transport. *Biochim. Biophys. Acta* **1767**, 1252–1259.
- Nandi, D.L., Horowitz, P.M. and Westley, J. (2000) Rhodanese as a thioredoxin oxidase. *Int. J. Biochem. Cell Biol.* **32**, 465–473.
- Nelson, N. and Yocum, C.F. (2006) Structure and function of photosystem I and II. *Annu. Rev. Plant Biol.* **57**, 521–565.
- Noctor, G. (2006) Metabolic signalling in defence and stress: the central roles of soluble redox couples. *Plant Cell Environ.* **29**, 409–425.
- Okutani, S., Hanke, G.T., Satomi, Y., Takao, T., Kurisu, G., Suzuki, A. and Hase, T. (2005) Three maize leaf ferredoxin:NADPH oxidoreductases vary in subchloroplast location, expression, and interaction with ferredoxin. *Plant Physiol.* **139**, 1451–1459.
- Palatnik, J.F., Valle, E.M. and Carrillo, N. (1997) Oxidative stress causes ferredoxin–NADP⁺ reductase solubilization from the thylakoid membranes in methyl viologen-treated plants. *Plant Physiol.* **115**, 1721–1727.
- Palatnik, J.F., Tognetti, V.B., Poli, H.O., Rodriguez, R.E., Blanco, N., Gattuso, M., Hajirezaei, M.R., Sonnewald, U., Valle, E.M. and Carrillo, N. (2003) Transgenic tobacco plants expressing antisense ferredoxin–NADP(H) reductase transcripts display increased susceptibility to photo-oxidative damage. *Plant J.* **35**, 332–341.

- Pantoja-Uceda, D., López-Méndez, B., Koshiba, S. et al.** (2004) NMR assignment of the hypothetical rhodanese domain At4g01050 from *Arabidopsis thaliana*. *J. Biomol. NMR*, **29**, 207–208.
- Pantoja-Uceda, D., López-Méndez, B., Koshiba, S. et al.** (2005) Solution structure of the rhodanese homology domain At4g01050(175–295) from *Arabidopsis thaliana*. *Protein Sci.* **14**, 224–230.
- Peltier, J.B., Ytterberg, A.J., Sun, Q. and van Wijk, K.J.** (2004) New functions of the thylakoid membrane proteome of *Arabidopsis thaliana* revealed by a simple, fast, and versatile fractionation strategy. *J. Biol. Chem.* **279**, 49367–49383.
- Quiles, M.J. and Cuello, J.** (1998) Association of ferredoxin–NADP oxidoreductase with the chloroplastic pyridine nucleotide dehydrogenase complex in barley leaves. *Plant Physiol.* **117**, 235–244.
- Rodermel, S.** (2001) Pathways of plastid-to-nucleus signalling. *Trends Plant Sci.* **6**, 471–478.
- Rodriguez, R.E., Lodeyro, A., Poli, H.O., Zurbriggen, M., Palatnik, J.F., Tognetti, V.B., Tschiersch, H., Hajirezaei, M.R., Valle, E.M. and Carrillo, N.** (2007) Transgenic tobacco plants overexpressing chloroplastic ferredoxin–NADP(H) reductase display normal rates of photosynthesis and increased tolerance to oxidative stress. *Plant Physiol.* **143**, 639–649.
- Rudolph, J.** (2005) Redox regulation of the Cdc25 phosphatases. *Antioxid. Redox Signal.* **7**, 761–777.
- Sansom, M.S. and Weinstein, H.** (2000) Hinges, swivels and switches: the role of prolines in signalling via transmembrane alpha-helices. *Trends Pharmacol. Sci.* **21**, 445–451.
- Schägger, H., Cramer, W.A. and von Jagow, G.** (1994) Analysis of molecular masses and oligomeric states of protein complexes by blue native electrophoresis and isolation of membrane protein complexes by two-dimensional native electrophoresis. *Anal. Biochem.* **217**, 220–230.
- Scholl, R.L., May, S.T. and Ware, D.H.** (2000) Seed and molecular resources for *Arabidopsis*. *Plant Physiol.* **124**, 1477–1480.
- Schwacke, R., Schneider, A., Van Der Graaff, E., Fischer, K., Catoni, E., Desimone, M., Frommer, W.B., Flugge, U.I. and Kunze, R.** (2003) ARAMEMNON, a Novel Database for Arabidopsis Integral Membrane Proteins. *Plant Physiol.* **131**, 16–26.
- Shaodong, D., Friemann, R., Glauser, D.A., Bourquin, F., Manieri, W., Schürmann, P. and Eklund, H.** (2007) Structural snapshots along the reaction pathway of ferredoxin–thioredoxin reductase. *Nature*, **448**, 92–96.
- Sokolenko, A., Fulgosi, H., Gal, A., Altschmied, L., Ohad, I. and Herrmann, R.G.** (1995) The 64 kDa polypeptide of spinach may not be the LHCII kinase, but a lumen-located polyphenol oxidase. *FEBS Lett.* **371**, 176–180.
- Stengel, A., Benz, P., Balsera, M., Soll, J. and Bölder, B.** (2008) TIC62 redox-regulated translocon composition and dynamics. *J. Biol. Chem.* **283**, 6656–6667.
- Zhang, H., Whitelegge, J.P. and Cramer, W.A.** (2001) Ferredoxin:NADP⁺ oxidoreductase is a subunit of the chloroplast cytochrome *b₆f* complex. *J. Biol. Chem.* **276**, 38159–38165.